ChemComm

COMMUNICATION

View Article Online
View Journal | View Issue

Check for updates

Cite this: *Chem. Commun.*, 2023, 59, 6714

Received 13th March 2023,
Accepted 4th May 2023

DOI: 10.1039/d3cc01249b

rsc.li/chemcomm

Fluorescence detected circular dichroism (FDCD) of a stereodynamic probe†

Roberto Penasa,[a] Federico Begato,[a] Giulia Licini,[a] Klaus Wurst,[b] Sergio Abbate,[c] Giovanna Longhi[c] and Cristiano Zonta *[a]

The use of chiroptical techniques in combination with stereodynamic probes is becoming one of the leading strategies for chiral sensing. While in most of the reported studies circular dichroism (CD) is the adopted spectroscopic technique, examples regarding the use of vibrational CD (VCD), circularly polarized luminescence (CPL), and Raman optical activity (ROA) are emerging as innovative tools. In this communication, an anthracene-decorated tris(2-pyridylmethyl)amine zinc complex (TPMA) is reported for its capability to act as a chiral sensor using either CD or fluorescence detected circular dichroism (FDCD). The latter technique offers the unique possibility to determine the enantiomeric excess of a series of carboxylic acids at sensor concentrations down to 0.1 μM. Limitations and possibilities opened by the use of this methodology, in particular regarding the specificity of the probe in the presence of another contaminant, are discussed.

Novel chiral sensors are being continuously developed with the idea to integrate fast spectroscopic techniques with high-throughput synthesis.[1–3] In particular, the interest in the determination of the enantiomeric excess (ee) is expanding outside traditional chromatographic methods with the aid of novel supramolecular architectures acting as chiral sensors using circular dichroism (CD).[4–9] Recently, other chiroptical techniques (vibrational circular dichroism (VCD),[10–13] circularly polarized luminescence (CPL)[14–16] and Raman optical activity (ROA[17])) have also raised interest in the community due to some peculiar features and advantages that these "alternative" spectroscopies can offer. Fluorescence detected circular dichroism (FDCD) has also attracted the interest of the community studying sensors[18–22] and recently Bräse, Biedermann *et al.* reported the possibility to obtain strong chiroptical responses related to molecular recognition events also at low concentrations. FDCD, which measures the difference in fluorescence intensity for left and right circularly polarized excitation,[23] combines the known advantages of fluorescence (*e.g.* sensitivity and selectivity) and the possibility to get information on the different absorptions of circularly polarized light of the analyte.[24–26] In analogy to excitation fluorescence that represents the indirect measurement of absorption in the case of fluorescent compounds, FDCD spectroscopy can be defined as the excitation fluorescence counterpart of CD. It should also be noted that conversion of any CD spectrometer to the FDCD setup can be easily obtained by shifting the photomultiplier tube (PM) detector to a 90-degree geometry with respect to the direction of the excitation light beam. In this configuration, attention to artifacts should be paid; in fact, fluorescence anisotropy components may be present, either due to the instrumentation itself or due to photoselection.[27] Inspired by these recent results and opportunities offered by this technique, in this communication we planned to investigate the performance of FDCD chiral sensing for a fluorescent stereodynamic probe. In particular, *tris*(2-pyridylmethyl)amine (**TPMA**) has been decorated with a fluorescent anthracene unit in order to act as an FDCD sensor. **TPMA** complexes, as a consequence of the propeller-like arrangement of the ligand around the metal center, have been extensively exploited by us[8,9,13,14] and others[28–30] as CD chiral probes for carboxylic acids due to their stereodynamic nature.[31,32] We report the fluorescent version of these systems, which undoubtedly enhances their sensing capabilities opening the possibility to use this type of sensing at very low sensor concentrations.

A fluorescent version of a **TPMA** probe was made by adding an anthracene moiety to the ligand skeleton (Fig. 1a). Our initial interest was to test if the simple incorporation of a fluorophore within a stereodynamic unit was sufficient for the development of an FDCD chiral sensor and to compare the potential of this technique with standard CD. The synthesis has been based on a procedure similar to those we already

[a] *Dipartimento di Scienze Chimiche Università degli Studi di Padova, via Marzolo 1, Padova 35131, Italy. E-mail: cristiano.zonta@unipd.it*
[b] *Department of General, Inorganic and Theoretical Chemistry University of Innsbruck, Innsbruck A-6020, Austria*
[c] *Department of Molecular and Translational Medicine Università degli Studi di Brescia Viale Europa 11 - 25123 Brescia – BS (Italy) and Istituto Nazionale di Ottica (INO), CNR, Research Unit of Brescia, via Branze 45, Brescia 25123, Italy*

† Electronic supplementary information (ESI) available. CCDC 2195380. For ESI and crystallographic data in CIF or other electronic format see DOI: https://doi.org/10.1039/d3cc01249b

Open Access Article. Published on 04 May 2023. Downloaded on 2/4/2026 7:08:58 AM. This article is licensed under a Creative Commons Attribution-NonCommercial 3.0 Unported Licence.

This journal is © The Royal Society of Chemistry 2023

Open Access Article. Published on 04 May 2023. Downloaded on 2/4/2026 7:08:58 AM.
This article is licensed under a Creative Commons Attribution-NonCommercial 3.0 Unported Licence.

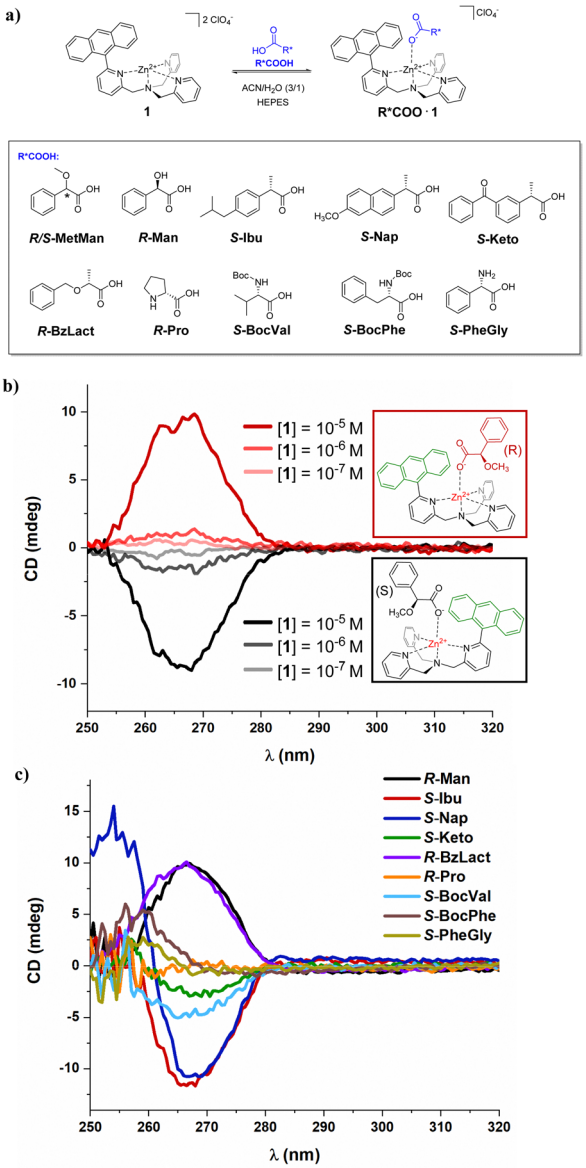

Fig. 1 (a) Complexation equilibria between the zinc complex **1** and the ten tested carboxylate species, (b) CD spectra superposition at different concentrations of the host **1** (10^{-5} M, 10^{-6} M, and 10^{-7} M) and the guests ***R*-MetMan** (red) and ***S*-MetMan** (black) at a concentration of 5×10^{-4} M (experiment performed at [**1**] = 10^{-7} M showed a residual signal due to the chiral acid itself), and (c) CD spectra superposition of the host **1** at a concentration of 10^{-5} M with the nine carboxylates tested at a concentration of 5×10^{-4} M.

described, which take advantage of the formation of a monobromo substituted ligand followed by the addition, *via* Suzuki–Miyaura coupling, of the anthracene unit (Section 3, ESI†). The resulting ligand after purification was solubilized in acetonitrile and one equivalent of zinc perchlorate hexahydrate was added. The zinc complex **1** was then precipitated by slow diffusion of diethyl ether to yield a yellow solid. Beside the classical NMR and MS characterizations (Fig. S6–S8, ESI†), the UV-Vis spectrum of **1** has been recorded and presents an intense band at 248 nm relative to the pyridyl systems and another one displaying the anthracene characteristic pattern at 345–395 nm (Fig. S9, ESI†). Interestingly, fixing excitation at 252 nm, the emission band of the anthracene substituent centred at 450 nm was observed (Fig. S13, ESI†).

Circular dichroism sensing: The capability of **1** to bind carboxylic acids and to amplify the chiroptical signal has been tested using as solvent an HEPES buffer solution (75% acetonitrile, 25% water) as reported by Anslyn *et al.* for similar systems.[33] This buffer allows control of the pH and consequently deprotonation and coordination of the carboxylate anion to the zinc complex. In more detail, a 10^{-5} M solution of complex **1** has been prepared in this solvent and additional aliquots of chiral (*R*)-(−)-methoxyphenylacetic acid, ***R*-MetMan**, added. CD titration spectra collected between 250 nm and 320 nm exhibit a strong positive signal centered at 268 nm, which increases up to 5.0 equivalents (Fig. S18, ESI†). Addition of excess chiral acid did not affect the final intensity of the signal. As expected, the mirror-image CD spectrum is obtained when (*S*)-(−)-methoxyphenylacetic acid, ***S*-MetMan**, is used. This is in line with previously examined systems in which enhancement of the dichroic signal arises from the preferential formation of a single propeller-like arrangement of **1**.

CD spectra were also recorded at different concentrations of sensor **1** keeping the concentrations of carboxylic acids ***R*-MetMan** and ***S*-MetMan** constant (Fig. 1b). As expected, CD showed a continuous decrease of the signal intensities, rapidly fading (from 10 to 0.1 mdeg within the range of 10^{-5}–10^{-7} M). Chiral sensing capabilities were also tested with nine other chiral carboxylic acids (Fig. 1c). In particular, the CDs of three non-steroidal anti-inflammatory drugs (ibuprofen ***S*-Ibu**, naproxene ***S*-Nap** and ketoprofen ***S*-Keto**), two Boc-protected amino acids (N-Boc-L-valine ***S*-BocVal** and Boc-L-α-phenylalanine ***S*-BocPhe**), two amino acids (proline ***R*-Pro** and phenylglycine ***S*-PheGly**), mandelic acid (***R*-Man**) and *O*-benzyl-D-lactic acid (***R*-BzLact**) were recorded. These acids, at a concentration of 5×10^{-4} M that simulates the concentration of a typical reaction mixture, have been tested at a probe concentration of 10^{-5} M and acids ***S*-Ibu**, ***S*-Nap**, ***R*-Man** and ***R*-BzLact** gave the most intense CD signals. On the other hand, ***R*-Pro** is much less intense, but still visible suggesting the involvement of the aromatic group in the sensing amplification (*viz.* either in the preferential helix formation or in the absorption process). Even if a preliminary observation suggests that all *R* acids have a positive band in the 270 nm region, and the opposite is observed for the *S* acids, the small dataset explored did not allow the description of a general structural model.

Fluorescence detected circular dichroism sensing: The chiroptical experiments were repeated changing the instrument to the FDCD setup. This mainly consists of the shift of the detector to a 90° geometry with respect to the incoming circularly polarized light beam. Moreover, a 420 nm long-pass filter was placed between the sample and the PM detector to avoid possible artefacts from scattered light. As done for CD, titration was carried out by adding to a 10^{-4} M solution of complex **1** additional aliquots of the chiral acid ***R*-MetMan** (Fig. S23, ESI†). Spectra were acquired using incident light from 250 nm to

Open Access Article. Published on 04 May 2023. Downloaded on 2/4/2026 7:08:58 AM.
This article is licensed under a Creative Commons Attribution-NonCommercial 3.0 Unported Licence.

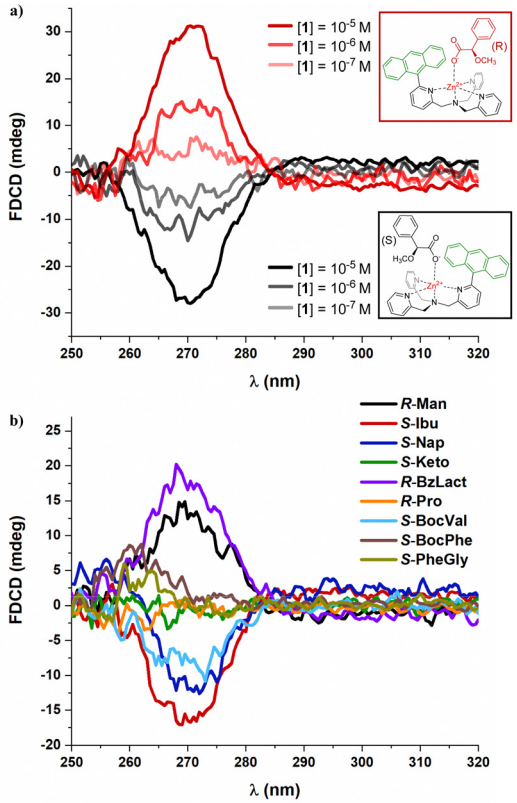

Fig. 2 (a) FDCD spectra superposition at different concentrations of host 1 and guests ***R*-MetMan** (red) and ***S*-MetMan** (black) at a concentration of 5×10^{-4} M. The HT(V) voltage was adjusted to the values 550 V, 690 V, and 790 V for the measurements at host concentration 10^{-5} M, 10^{-6} M, and 10^{-7} M, respectively; b) FDCD spectra superposition of the host 1 at a concentration of 5×10^{-6} M with the nine carboxylates tested at concentrations of 5×10^{-4} M (HT = 570 V). Meaningful FDCD signals can be obtained also at lower analyte concentration according to the binding constant (Fig. S21, ESI†).

320 nm and by recording the FDCD signals and the total fluorescence (DC(V)) simultaneously. One band centered at 275 nm appeared upon addition of the chiral acid. Interestingly, at higher wavelengths, a less intense and broadened band appeared during the titration process (Fig. S23, ESI†). To test the potential higher sensitivity achieved with the fluorescence technique, FDCD measurements were recorded at different concentrations of the sensor **1** within the range of 10^{-5}–10^{-7} M keeping the concentration of the carboxylic acids ***R*-MetMan** and ***S*-MetMan** constant (Fig. 2a). Within the analyzed range, the high voltage (HT(V)) of the PM detector was adjusted to 550 V, 690 V and 790 V values, respectively, for the 10^{-5} M, 10^{-6} M, and 10^{-7} M concentrations. This was necessary in order to optimize the total fluorescence (DC(V)) of the instrument. Similar to CD, the FDCD signal decreases with dilution of the host. However, while CD fades very rapidly, the FDCD response retains a meaningful signal up to 10^{-7} M (~5 mdeg). Also in the case of FDCD, measurements were performed for the other nine chiral carboxylic acids (Fig. 2b). These acids have been tested at a host concentration of 5×10^{-6} M. Also in this case the acids ***S*-Ibu**, ***S*-Nap**, ***R*-Man** and ***R*-BzLact** gave the most intense chiroptical signals. As expected, the dichroism output obtained with the two techniques is comparable. An exception is represented by the ***S*-Keto** acid that shows a flat FDCD signal beside the CD signal. This is likely due to fluorescence quenching of the complex upon the addition of the acid as indicated by the absence of signal in the total fluorescence response.

FDCD may show good accessibility to signals that are very weak at CD, thus possibly extending the spectroscopic range useful for sensing. In the case herein examined, at high host concentration ([**1**] = 10^{-4} M), it is possible to detect a non-zero broad signal in the range of 290–350 nm (see Fig. S23, ESI†). This signal is also observed in the CD spectrum at higher concentration (see Fig. S19, ESI†), and is more easily readable in the FDCD case, showing higher relative intensity compared to the 270 nm band that in this case is lowered by auto-absorption.

As a proof of the higher sensitivity of FDCD in comparison with CD, a calibration line was built for both techniques using samples of known enantiopurity. While in the case of FDCD a good linear fit was observed at sensor concentrations of 10^{-7} M, in the case of CD linearity is less evident due to the high noise/signal ratio particularly at low e.e. (Fig. S20 and S24, ESI†). Specificity of the probe in the presence of a "chiroptical contaminant" was also tested. In particular, we devised an experiment in which keeping constant in solution the concentration of the couple **1** and ***R*-MetMan**, increasing amounts of ***R*-BINAPO** were added. ***R*-BINAPO** was chosen because it has substantial chiroptical activity (see Fig. S22, ESI†) in the whole spectroscopic region investigated in these experiments. As expected, while the chiroptical activity of ***R*-BINAPO** strongly influences the CD spectra, FDCD remains unaffected (Fig. 3). In other words, while the CD intensity at 275 nm cannot be directly correlated to enantiomeric excess of the analyte, FDCD is transparent to the contaminant. On the other hand, as expected, the addition of a chiral fluorescent "contaminant" has a sensible effect on the FDCD signal (Fig. S27, ESI†).

Structural details on the recognition of the chiral carboxylic acids were obtained from the crystallographic analysis of a single crystal prepared by slow evaporation of an acetonitrile solution containing a stoichiometric amount of **1** and ***R*-MetMan** (Fig. 4).

It is possible to notice an edge-to-face interaction between the phenyl group of the ***R*-MetMan** acid and one of the

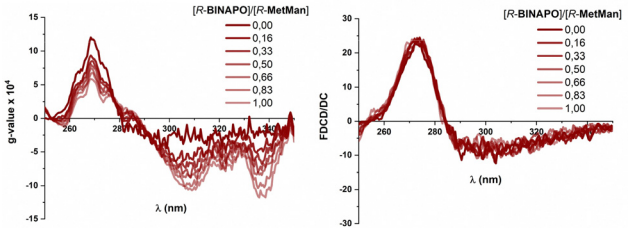

Fig. 3 (a) g-values and (b) FDCD/DC signals of the titration of the host **1** (10^{-5} M) and ***R*-MetMan** (5×10^{-4} M) with additional aliquots of ***R*-BINAPO** (from 0 M (solid line) to 5×10^{-4} M (faded line)) (see also Fig. S16 and S20, ESI†).

 This journal is © The Royal Society of Chemistry 2023

Open Access Article. Published on 04 May 2023. Downloaded on 2/4/2026 7:08:58 AM.
This article is licensed under a Creative Commons Attribution-NonCommercial 3.0 Unported Licence.

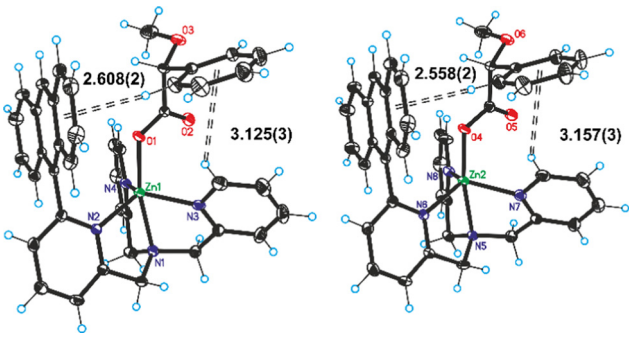

Fig. 4 Ortep plots of the two independent cationic Zn-complexes in the asymmetric unit. Thermal ellipsoids are shown at the 30% probability level and the distances of π–H interactions in Å. Triethylammonium cations and perchlorate anions present in the cell have been removed for clarity.

unsubstituted pyridine rings of the complex **1**. A second interaction between the phenyl ring of ***R*-MetMan** and the anthracene group of **1** is also clearly visible. More importantly, a single helicity of the **TPMA** unit is observed along the crystal packing (Fig. S29 and S30, ESI†). Comparison between experimental and calculated CD spectra was carried out. Theoretical calculations with time-dependent DFT (TD-DFT) method were conducted at the M06/6-311+g(*d*,*p*) level. The most populated conformer (77% population) is quite similar to the crystal structure reported above. The CD spectra have been calculated for three conformers of ***R*-MetMan** hosted in **1** and the average spectrum thereof is presented in Fig. S33, ESI.† Good correspondence is found with experimental data. Analysis of the electronic transitions responsible for the observed signals is illustrated in the ESI† showing large contributions from the anthryl moiety to all intense features. In particular, the band observed at 250 nm (that is, at the irradiation wavelength used for obtaining fluorescence spectra) contains two main contributions involving not only the anthryl moiety but also the pyridine groups and the phenyl of the chiral acid (transitions 50 and 51 of Table S1, ESI†). The same transitions contribute to the positive CD band together with slightly lower energy transitions, the most intense one being #46 of Table S1 (ESI†), which involves also the phenyl ring: altogether these transitions account for the CD band observed at 265 nm.

The combination of a stereodynamic system based on **TPMA** with a fluorescent molecule has been shown to be a molecular sensor able to act as a probe for chiral carboxylic acids using CD and FDCD. The latter technique is found to be more accurate and sensitive for the determination of the enantiomeric excess also at very low concentrations and insensitive to the presence of chiral contaminants. It should be noted that contaminants should not interact with the probe or have fluorescence activity in the same spectroscopic region. This fact gives the possibility of disentangling two overlapping CD species. This simple design can lead to the development of novel chemical sensors.

University of Padova (P-DiSC#10 BIRD2020-UNIPD), Fondazione CARIPARO (Chiralspace) and MUR (PRIN 2017 2017A4XRCA_003) are acknowledged for funding.

Conflicts of interest

There are no conflicts to declare.

References

1 G. Pescitelli, D. Bari and N. Berova, *Chem. Soc. Rev.*, 2014, **43**, 5211–5233.
2 D. Leung, S. O. Kang and E. V. Anslyn, *Chem. Soc. Rev.*, 2012, **41**, 448–479.
3 M. Quan, X. Y. Pang and W. Jiang, *Angew. Chem., Int. Ed.*, 2022, **61**(1–14), e202201258.
4 J. R. Howard, A. Bhakare, Z. Akhtar, C. Wolf and E. V. Anslyn, *J. Am. Chem. Soc.*, 2022, **144**, 17269–17276.
5 A. Sripada, F. Yushra, C. Wolf, A. Sripada, F. Y. Thanzeel and C. Wolf, *Chemistry*, 2022, **8**, 1734–1749.
6 D. S. Hassan and C. Wolf, *Nat. Commun.*, 2021, **12**, 1–10.
7 Z. A. De Los Santos, L. A. Joyce, E. C. Sherer, C. J. Welch and C. Wolf, *J. Org. Chem.*, 2019, **84**, 4636–4645.
8 F. Begato, R. Penasa, G. Licini and C. Zonta, *ACS Sens.*, 2022, **7**, 1390–1394.
9 F. A. Scaramuzzo, G. Licini and C. Zonta, *Chem. – Eur. J.*, 2013, **19**, 16809–16813.
10 G. Tino, K. Taichi, M. Keiji and C. Merten, *Chem. Commun.*, 2022, **58**, 8412–8415.
11 M. Kemper, E. Engelage and C. Merten, *Angew. Chem. – Int. Ed.*, 2021, **60**, 2958–2962.
12 R. Berardozzi, E. Badetti, N. A. Carmo Dos Santos, K. Wurst, G. Licini, G. Pescitelli, C. Zonta and L. Di Bari, *Chem. Commun.*, 2016, **52**, 8428–8431.
13 C. Bravin, G. Mazzeo, S. Abbate, G. Licini, G. Longhi and C. Zonta, *Chem. Commun.*, 2022, **58**, 2152–2155.
14 N. A. Carmo dos Santos, E. Badetti, G. Licini, S. Abbate, G. Longhi and C. Zonta, *Chirality*, 2018, **30**, 65–73.
15 J. Gong and X. Zhang, *Coord. Chem. Rev.*, 2022, **453**, 214329.
16 K. Omasa, M. Ito and Y. Kubo, *New J. Chem.*, 2022, **46**, 21845–21851.
17 E. Machalska, N. Hachlica, G. Zajac, D. Carraro, M. Baranska, G. Licini, P. Bouř, C. Zonta and A. Kaczor, *Phys. Chem. Chem. Phys.*, 2021, **23**, 23336–23340.
18 A. Belardini, E. Petronijevic, R. Ghahri, D. Rocco, F. Pandolfi, C. Sibilia and L. Mattiello, *Appl. Sci.*, 2021, **11**, 1–8.
19 Z. Dai, G. Proni, D. Mancheno, S. Karimi, N. Berova and J. W. Canary, *J. Am. Chem. Soc.*, 2004, **126**, 11760–11761.
20 A. Prabodh, Y. Wang, S. Sinn, P. Albertini, C. Spies, E. Spuling, L. P. Yang, W. Jiang, S. Bräse and F. Biedermann, *Chem. Sci.*, 2021, **12**, 9420–9431.
21 T. Nehira, C. A. Parish, S. Jockusch, N. J. Turro, K. Nakanishi and N. Berova, *J. Am. Chem. Soc.*, 1999, **121**, 8681–8691.
22 T. Nehira, K. Ishihara, K. Matsuo, S. Izumi, T. Yamazaki and A. Ishida, *Anal. Biochem.*, 2012, **430**, 179–184.
23 I. Tinoco and D. H. Turner, *J. Am. Chem. Soc.*, 1976, **98**, 6453–6456.
24 K. Tanaka, G. Pescitelli, K. Nakanishi and N. Berova, *Monatsh. Chem.*, 2005, **136**, 367–395.
25 D. H. Turner, I. Tinoco Jr and M. Maestre, *J. Am. Chem. Soc.*, 1974, **769**, 4340–4342.
26 J. G. Dong, A. Wadas, T. Takakuwa, K. Nakanishi and N. Berova, *J. Am. Chem. Soc.*, 1997, **119**, 12024–12025.
27 E. Castiglioni, S. Abbate, F. Lebon and G. Longhi, *Methods Appl. Fluoresc.*, 2014, **2**, 024006.
28 C. Bravin, E. Badetti, G. Licini and C. Zonta, *Coord. Chem. Rev.*, 2021, **427**, 213558.
29 L. A. Joyce, J. W. Canary and E. V. Anslyn, *Chem. – Eur. J.*, 2012, **18**, 8064–8069.
30 L. You, G. Pescitelli, E. V. Anslyn and L. Di Bari, *J. Am. Chem. Soc.*, 2012, **134**, 7117–7125.
31 C. Wolf and K. W. Bentley, *Chem. Soc. Rev.*, 2013, **42**, 5408–5424.
32 K. W. Bentley and C. Wolf, *J. Org. Chem.*, 2014, **79**, 6517–6531.
33 L. A. Joyce, M. S. Maynor, J. M. Dragna, G. M. Da Cruz, V. M. Lynch, J. W. Canary and E. V. Anslyn, *J. Am. Chem. Soc.*, 2011, **133**, 13746–13752.